Journal of Sound and Vibration (1997) **208**(2), 299–311

VIBRATION CONTROL FOR A HIGH-Tc SUPERCONDUCTING NON-LINEAR LEVITATION SYSTEM

K. NAGAYA, M. TSUKAGOSHI AND Y. KOSUGI

Department of Mechanical Engineering, Gunma University, Kiryu, Gunma 376, *Japan*

AND

M. MURAKAMI

Superconductivity Research Laboratory, Sinonome, Tokyo, 135, *Japan*

(*Received* 10 *February* 1997, *and in final form* 4 *July* 1997

In the present paper the modelling and control of a high-Tc superconducting levitation system are discussed. First, the analytical expressions for obtaining the non-linear levitation force, given by the present author, are clarified; and then a vibration control method is presented in which feedback currents involving frequency weights are used. In the method, the square of the displacement in the frequency domain is taken as a cost function. Optimal coefficients of the transfer function of the controller are obtained by minimizing the cost function. Hence, the spillover instability due to the non-linear vibrations will be reduced. Numerical calculations have been carried out for some typical problems. To validate the present method, experimental tests have also been carried out.

1. INTRODUCTION

Recently, large pieces of high-Tc superconductor bulk material with high critical currents have been produced [1, 2]. Since the superconducting levitation system has a large pinning force in comparison with its volume, the system is stable in both the horizontal and the vertical directions, so that it has been applied to various fields [3]. Knowledge of the levitation force is required in order to design a levitation system, and so a number of studies for a static levitation force have been reported [4–8]. In the dynamic problem when the superconductor vibrates in a magnetic field, there are two regions of flux creep and flux flow, so the dynamic characteristic is different from the static one. For the dynamic problem, Yoshida, Uesaka and Miya [9] have presented a numerical method. The present author also gave an approximate analysis for obtaining the dynamic levitation force, and it was clarified that the dynamic levitation force is dependent on the air gap, the vibration amplitude and the vibration frequency [10]. A method of modelling for a thick circular conductor also has been reported by the present author [11].

The vibration control problem of high-Tc superconducting levitation system is of importance, and the present authors have discussed vibration isolation control theoretically by using the PD control for a thin superconducting disc under low frequency excitations [10]. However, since the system has non-linear behavior, the PD control is not valid for controlling the levitation body in a large frequency region. In particular, the calculation becomes significantly large when the equation in reference [10] is used, because the equation of motion of the system is combined with the analysis of the non-linear

0022–460X/97/470299 + 13 $25.00/0/sv971223

levitation force. Hence it is difficult to obtain a frequency response by using this equation. Owing to the background as mentioned above, although the present authors have discussed the modelling of the system, the method has not been certified. Hence the present paper discusses the validity of the modelling at the first step, then a vibration control method for the levitated body is presented, with consideration of the non-linear behavior over a wide frequency zone, including the subharmonic, harmonic and superharmonic zones. Although the system is a single-degree-of-freedom system, a number of non-linear modes will be generated, and so a spillover instability will be generated, which is often observed in flexible structures when the controller is designed by using a linear system.

In the present paper, a vibration control method is set out in which feedback currents involve frequency weights. In the method, the square of the displacement in a frequency domain is taken as a cost function. Optimal coefficients of the transfer function of the controller are obtained by minimizing the cost function. The spillover instability due to the non-linear phenomena will then be reduced. Numerical calculations are carried out for the response of the levitated body under the control. To validate the theoretical analysis, experimental tests are also carried out.

2. THEORETICAL AND EXPERIMENTAL RESULTS FOR THE LEVITATION FORCE

2.1. THEORETICAL LEVITATION FORCE

The geometry of the high-Tc superconducting levitaton system treated in the present paper is illustrated in Figure 1. A cylindrical permanent magnet attached to a circular electromagnet is levitated by a pinning force of the superconductor which lies on the base. In this system, when a current is applied in the coil of an electromagnet consisting of a ferrite core with a coil, magnetic flux densities vary, and so the levitation forces vary. The magnetic flux densities due to the permanent magnet with the electromagnet are reported in reference [13] as

$$B_r = B_{pr}(r, z) + B_{ecr}(r, z, I) + B_{esr}(r, z, I), \tag{1a}$$

$$B_z = B_{pz}(r, z) + B_{ecz}(r, z, I) + B_{esz}(r, z, I), \tag{1b}$$

where r and z denote the co-ordinates and I is the control current. A method of calculation of a levitation force has been given in our previous report [11], but experimental tests have not been previously carried out. In this paper, the authors' analytical results are discussed by comparing the theoretical results with the experimental data.

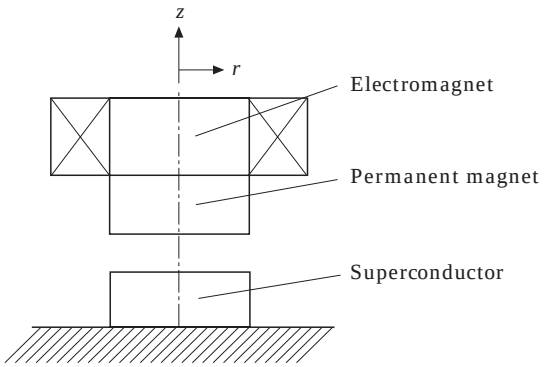

Figure 1. The analytical model.

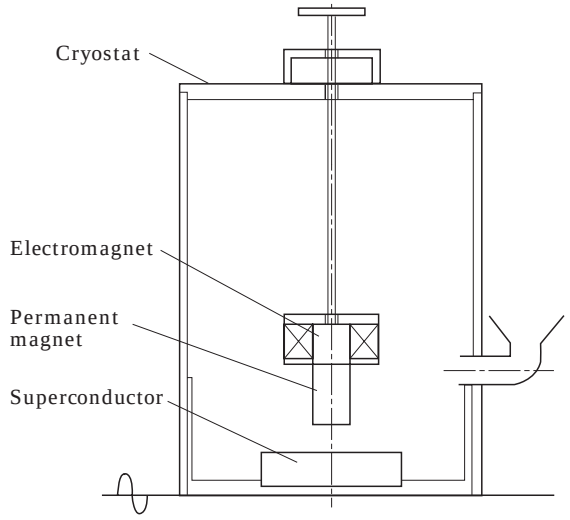

Figure 2. The geometry of the experimental apparatus.

The vector potential $A(r, z)$ in the conductor is [11]

$$A(r, z) = \frac{2\mu_0}{l} \sum_{j=1}^{N'} \sum_{i=1}^{N} \sum_{n=0}^{\infty} \varepsilon_n J_{ji} r_i \Delta r_i \Delta z_j D_{ni}(r) \cos \frac{n\pi z_j}{l} \cos \frac{n\pi z}{l}, \tag{2}$$

where Δr_i is the element length in the r-direction, Δz_j is the element length in the z-direction, r_i and z_i are the co-ordinates at the ith circle and jth sections, respectively, J_{ji} is the shield current density at the (j, i)th circle in the conductor, N' is the number of divisions in the z-direction, N is the number of divisions in the r-direction, and the $D_{ni}(r)$ are given in reference [11]. The current density J_{ji} is obtained by the following equations:

$$f_{ji}(J_{ji}) + \left\{ \frac{A_{sji}(T) - A_{sji}(T - \Delta t)}{\Delta t} \right\} = 0, \qquad j = 1, 2, \ldots, N', \quad i = 1, 2, \ldots, N, \tag{3}$$

TABLE 1

Dimensions of the superconductor and magnet

Radius of the permanent magnet	12 mm
Thickness of the permanent magnet	20 mm
Magnetization strength of the permanent magnet	0·88 T
Inner radius of the coil	12 mm
Outer radius of the coil	26·8 mm
Thickness of the coil	12·8 mm
Turn of the coil	155
Radius of the core	12 mm
Thickness of the core	14·8
Diameter of the high-Tc superconductor	49·3 mm
Thickness of the superconductor	13·8 mm
Pinning potential, U_0	92×10^{-3} eV
Critical electric field, $E_c = \rho_c J_c$	$0{\cdot}1 \times 10^{-3}$ V/m
Temperature, θ	77 K
Initial air gap, d	2 mm

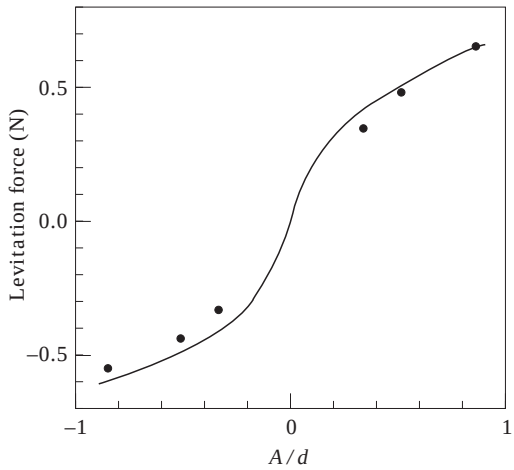

Figure 3. A comparison between theoretical (—) and experimental (●) levitation forces.

TABLE 2

Coefficient of the approximate equation for the levitaton force

$a_1 =$	1·624068
$a_2 =$	$1{\cdot}614288 \times 10^{-2}$
$a_3 =$	-3.042525
$a_4 =$	4.694524×10^{-2}
$a_5 =$	2·683826
$a_6 =$	$3{\cdot}410975 \times 10^{-3}$

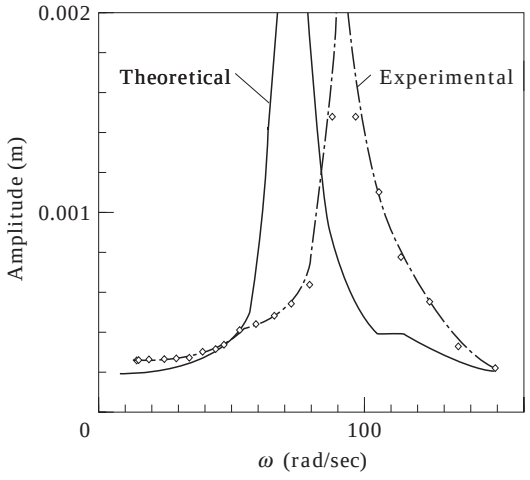

Figure 4. A comparison between theoretical (—) and experimental (– –◇– –) frequency response curves.

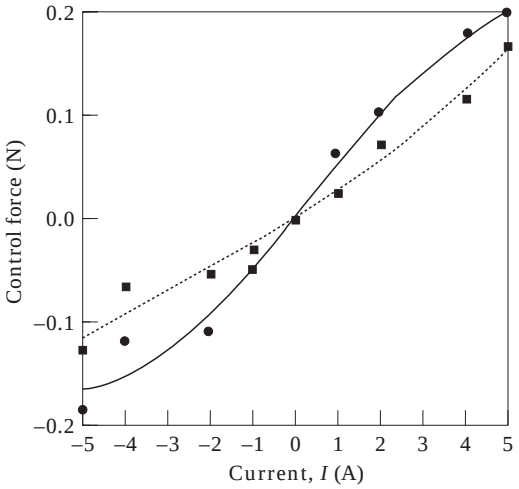

Figure 5. Control forces versus control currents obtained by the experiment. —, ●, $A/d = 0{\cdot}1$; ····, ■, $A/d = 0{\cdot}5$.

where T is the time, Δt is the incremental time from T, and $A_{ji}(T)$ is the vector potential $A(r_i, z_j)$ on the (j, i)th circle at time T. In the calculation of equation (3), the following constitutive equations are used:

$$f(J) = E = 2\rho_c J_c \sinh\left(\frac{U_0}{k\theta}\frac{J}{J_c}\right)\exp\left(-\frac{U_0}{k\theta}\right) \qquad \text{for } |J| \leqslant J_C,$$

$$f(J) = E = E_c + \rho_f J_c(J/J_c - 1) \qquad \text{for } |J| > J_C, \tag{4}$$

where E is the electric field, θ is the temperature (in K), U_0 is the pinning potential, k is the Boltzmann constant, ρ_c is the flux creep resistance, ρ_f is the flux flow resistance, J_c is the critical current density and $E_C = \rho_c J_c$. By using equations (1)–(4), the shield currents J_{ji} can be calculated. Then the levitation force is obtained from the following equation:

$$F = \sum_{j=1}^{N'}\sum_{i=1}^{N} 2\pi r_i J_{ji}\Delta r_i \Delta z_i B_{rji}. \tag{5}$$

TABLE 3

Optimal coefficients of the controller

Coefficients	Before optimization	After optimization
c_1	1·0	1·0
c_2	1·0	1·1
d_1	1.0×10^3	$8{\cdot}9 \times 10^3$
d_2	1.0×10^3	$5{\cdot}9 \times 10^3$
e_1	1·0	1·0
e_2	1·0	1·2
g_1	$1{\cdot}0 \times 10^3$	$8{\cdot}7 \times 10^2$
g_2	$1{\cdot}0 \times 10^3$	$7{\cdot}3 \times 10^2$

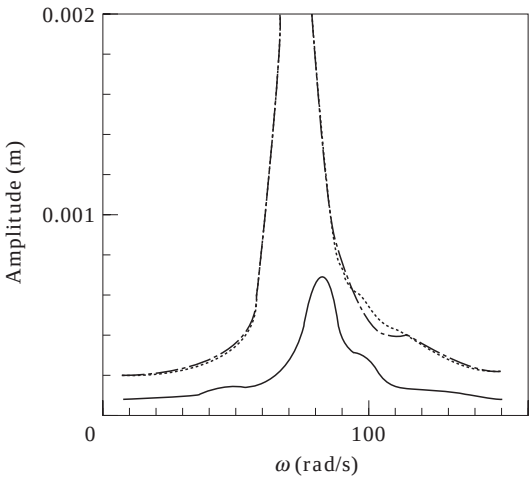

Figure 6. Theoretical frequency response curves with or without control. –·–, without control; ····, before optimization; —, after optimization.

2.2. EXPERIMENTAL LEVITATION FORCE

An experimental set-up for obtaining the levitation force, in which a solid cylindrical high-Tc superconductor lies on the base, and a cylindrical permanent magnet attached to an electromagnet is levitated, is illustrated in Figure 2. To detect the displacement of the magnet, a solid straight bar made of copper is attached to the electromagnet, which is passing through the cryostat as shown in Figure 2. When the levitation force is measured, an aluminum bar with the other end built-in is pin-joined to the top of a copper bar at right-angles. A strain gauge attached to the surface of the aluminum bar detects strains when the force is produced between the permanent magnet and the superconductor. The superconductor and magnets are inserted in a cylindrical cryostat made of aluminum, and cooled inside by liquid nitrogen. The cryostat lies on the oscillator, and so the levitation force varies when the oscillation $(u = A \sin \omega t)$ is applied to the cryostat.

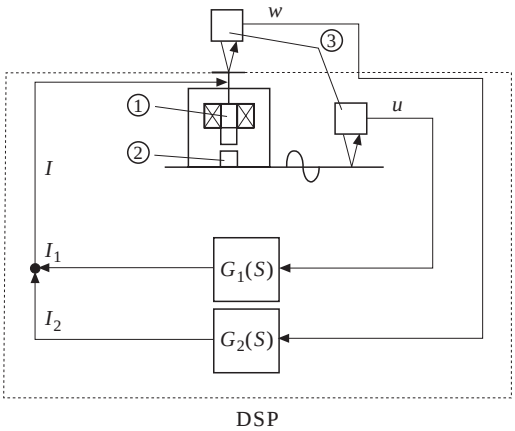

Figure 7. The block diagram of the present control system. ①, Actuator; ②, superconductor; ③ laser gap sensor.

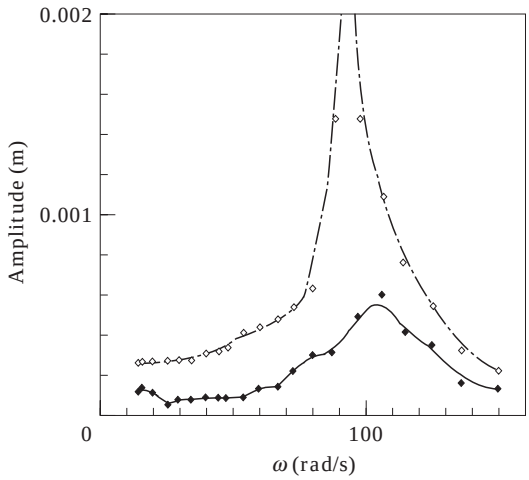

Figure 8. Frequency response curves with (—◆—) or without (– – ◇ – –) control obtained by the experiment.

In this experimental set-up, both the superconductor and magnet lie in the cryostat, so the superconductor is affected by the magnet. Strictly speaking, the conductor is cooled in a magnetic field. The velocity of the magnet is important when the magnet is put on the superconductor [9, 11], but it is difficult to move the magnet with the same velocity. Hence, in the present experiment, the magnet is locked with a certain air gap, and the lock is loosened after cooling. This implies that the magnet falls freely by the force of gravity, and the condition of the levitation becomes always constant. When the lock is loosened after cooling, the magnet is levitated to an equilibrium position in which the force of gravity is equal to the levitation force. There are static shield currents inside the conductor after levitating the magnet. In addition, there is the effect of the magnetic field cooling, but this will be small when the air gap is large. When the magnet vibrates from the equilibrium position, the total current inside the conductor is given by the addition of the static current and the dynamic current. If the total current is less than the critical current, the motion of the levitated body is in the flux creep region, but it is in the flux flow region when the total current is greater than the critical current. Then, strictly speaking, the levitation force of the system should be obtained by considering all routes from the cooled position. In the calculation of the force, however, the calculation technique becomes significantly complex, and the calculation error for the dynamic levitation force increases when the static levitation force is large in comparison with the dynamic force. For the reasons just mentioned, in the present paper the dynamic levitation force is considered only from static equilibrium. In this case, the critical current should be varied with consideration of the static shield current. The equivalent critical current and flux flow resistance during vibration are determined by reference to the experimental data. The experimental tests were carried out for the following case: mean air gap (air gap at the static equilibrium position), $d = 2$ mm; amplitudes of vibration displacements $A = 1{\cdot}69$ mm, $1{\cdot}02$ mm and $0{\cdot}68$ m (three cases); frequency $\omega = 8{\cdot}8$ rad/s. The dimensions of the superconductor and the magnet are depicted in Table 1. The material constants of the superconductor were assumed to have the same values as in reference [11], but the flux flow resistance and critical current (without the effects of the magnetic flux) were determined in the same way as in reference [11]. Those values were $\rho_f = 2{\cdot}5 \times 10^{-10}\Omega$ m and $J_{c0} = 1{\cdot}5 \times 10^6 A/m^2$. A comparison between the theoretical result and the experimental data for the restoring force during vibration is shown in Figure 3. The theoretical result (the solid line in Figure 3)

almost coincides with the experimental data (the black dot). This implies that our approximate analysis seems to be valid for calculating the dynamic levitation force (restoring force) in high-Tc superconducting levitation system.

The following approximation is applicable for the curve in Figure 3:

$$F = \sum_{k=1}^{n} a_k (A/d)^k, \tag{6}$$

where F is the levitation force, A is the amplitude, d is the initial air gap, and the a_k are the coefficients as shown in Table 2, which are determined by the least squares method, by use of the theoretical curve in Figure 3. The restoring force also depends on the frequency; the result involving the effect of frequency can be obtained by use of the expression as just mentioned. However, it is difficult to give an approximate expression involving both the effects of amplitude and frequency. Hence, hereafter, a simple expression involving only the effect of amplitude given by equation (6) is used.

3. THEORETICAL AND EXPERIMENTAL RESULTS FOR FREQUENCY RESPONSE

When the base is excited by the displacement $u(t)$, the equation of motion of the levitated body is

$$m\frac{\mathrm{d}^2 w}{\mathrm{d}t^2} + c\left(\frac{\mathrm{d}w}{\mathrm{d}t} - \frac{\mathrm{d}u}{\mathrm{d}t}\right) + \sum_{k=1}^{n} a_k \left(\frac{w-u}{d}\right)^k = 0, \tag{7}$$

where m is the mass of the levitated body, c is the damping coefficient, w is the displacement of the levitated body and the third term in equation (7) the force between the superconductor and the levitation magnet. Equation (7) is the typical non-linear equation, and so it is difficult to solve it analytically. In the present paper, the numerical method (Runge–Kutta–Gill method) is applied.

The dimensions of the system used in the numerical calculations are as follows: the mass of the levitated body, $m = 0{\cdot}12$ kg; the damping coefficient, which was determined in the experiment, $c = 5{\cdot}5 \times 10^{-2}$ Ns/m; the amplitude of the base displacement, $u_0 = 0{\cdot}2$ mm; and the initial air gap at static equilibrium, $d = 2$ mm. The material constants and the dimensions of the superconductor and the magnet are the same as mentioned above. The time response curves are obtained by the Runge–Kutta–Gill method, and taking the amplitude at the steady state, we have the frequency response curves for this non-linear system. A solid line in Figure 4 shows the calculated frequency response curve. In the figure a non-linear vibration (superharmonic motion) is observed at a frequency two times the main resonance frequency.

Experimental tests were also carried out for the same model. In the experiment, the same apparatus as in Figure 2 was applied, but the magnet was levitated freely without constraint. The base of the cryostat was excited by the oscillator, and the displacement of the levitated body was measured by a non-contact displacement sensor (laser gap sensor). The results are plotted as open dots in Figure 4. The dynamic restoring force (levitation force) increases with increasing values of the frequency, but it reduces to a certain value when the frequencies become large. This implies that the resonance frequency of the superconducting levitation system increases in comparison with the usual non-linear system, which does not depend on the frequencies. For this reason, there are about ten percent errors between the theoretical resonance frequency and the experimental one. Hence the effects of the frequency on the restoring force should be considered in the design

of the controller, as mentioned below. Although the theoretical resonance frequency is somewhat smaller than the experimental one, the trends of both results are in good agreement.

4. VIBRATION CONTROL WITH CONSIDERATION OF NON-LINEAR PHENOMENA

The following assumptions are used in the design of the controller.

(1) Since the amplitude of vibration is large in this system, the non-linear effects on the restoring force are considered, and equation (6) is applied.

(2) Since the frequency depends on the restoring force, the resonance frequency in the theory will be small in comparison with that of the real superconducting levitation system. The controller is then designed with consideration of this phenomenon. In the present paper, a transfer function with frequency weighting is applied.

(3) There are also non-linear relations between the control currents and the restoring forces. The effect of non-linear phenomena between the amplitude and the restoring force is then considered, but the effect of the frequency is considered in the design of the controller. Strictly speaking, the levitation force involving the control current cannot be obtained by the addition of the force due to the permanent magnet and that due to the control current. In this system, however, the force due to the control current is small in comparison with that due to the permanent magnet. Then the total force is obtained by the addition of these two forces.

Under the assumptions just mentioned, the present system can be modelled as a single-degree-of-freedom system. Hence the equation of motion is denoted as the following non-linear equation:

$$m\frac{\mathrm{d}^2w}{\mathrm{d}t^2} + c\left(\frac{\mathrm{d}w}{\mathrm{d}t} - \frac{\mathrm{d}u}{\mathrm{d}t}\right) + \sum_{k=1}^{n} a_k\left(\frac{w-u}{d}\right)^k = -Q(A, d, I) + P, \tag{8}$$

where u is the displacement ($=u_0 \sin \omega t$), w is the displacement of the levitated body, Q is the control force, I is the control current and P is the load applied to the levitated body.

4.1. VIBRATION ISOLATION CONTROL BY USE OF THE FEEDBACK CONTROL WITH FREQUENCY WEIGHTING

The amplitude at the resonance frequency decreases with the velocity feedback coefficient, and the negative displacement feedback makes the system stiffness decrease, leading to a decrease in vibration transmission. However, since the system stiffness decreases, the system becomes unstable. For the reason just mentioned, the control is not desirable, and the displacement of the levitated body becomes greater than the base displacement in the low frequency region in the usual PID control. To decrease the vibration transmission in the low frequency region, the disturbance cancellation technique given by the present author [12] is straightforward to apply. The transmission can be reduced significantly (by one-third to a tenth) by making use of only the feedback of the base displacement in the disturbance cancellation method. Hence, in the present paper, both the vibration of the levitated body and the base are fed to the actuator. Since the system has non-linear behavior, as stated above, the theoretical resonance frequency will be somewhat different from that of the real system. The following function having frequency weighing is then used as a transfer function for the controller:

$$G_1(s) = \frac{d_1 s + d_2}{c_1 s + c_2}, \qquad G_2(s) = \frac{g_1 s + g_2}{e_1 s + e_2}, \tag{9}$$

where G_1 is the transfer function for the base disturbance, and G_2 is for the levitated body. By using equation (9), the gain can be controlled to be flat near the resonance frequency. Hence the current becomes

$$\bar{I}(s) = G_1(s)\bar{u}(s) + G_2(s)\bar{w}(s). \tag{10}$$

The equations of state are

$$\dot{y}_1 = y_2, \quad \dot{y}_2 = \frac{1}{m}\left[-Q(A, d, I) - \sum_{k=1}^{6} a_k \left(\frac{y_1 - u}{d}\right)^k - c(y_2 - \dot{u}) \right],$$

$$\dot{y}_3 = \frac{1}{c_1}[d_1\dot{u} + d_2 u - c_2 y_3], \qquad \dot{y}_4 = \frac{1}{e_1}[g_1 y_2 + g_2 y_1 - e_2 y_3], \tag{11}$$

where y_1 is the displacement of the levitated body, y_2 is the velocity of the levitated body, y_3 is the control current ($=I_1$) for the base disturbance, y_4 is the control current ($=I_2$) for the vibration of the levitated body, and c_1, c_2, d_1, d_2, e_1, e_2, g_1 and g_2 are the coefficients of the controller as shown in equation (9).

4.2. DESIGN OF CONTROLLER FOR THE LOAD APPLYING TO THE LEVITATED BODY

We consider a case in which a vibration force $P = P_0 \sin \omega t$ applies to the levitated body. Let the transfer function of the controller be

$$G_3(s) = \frac{p_1 s + p_2}{q_1 s + q_2} \tag{12}$$

and let the current be

$$\bar{I}(s) = G_3(s)\bar{w}(s) \tag{13}$$

in the same way as previously. The equation of state also becomes the following non-linear equations:

$$\dot{y} = y_2, \qquad \dot{y}_2 = \frac{1}{m}\left[-Q(A, d, I) - \sum_{k=1}^{6} a_k \left(\frac{y_1}{d}\right)^k - c y_2 + P_0 \sin \omega t \right],$$

$$\dot{y}_3 = \frac{1}{q_1}[p_1 y_2 + p_2 y_1 - q_2 y_3], \tag{14}$$

where y_1 is the displacement of the levitated body, y_2 is the velocity, y_3 is the control current ($=I_3$), and p_1, p_2, q_1 and q_2 are the coefficients of the transfer function, as shown in equation (12).

4.3. OPTIMIZATION OF THE TRANSFER FUNCTION OF THE CONTROLLER

The total control current applied to the coil is given by the addition of each current:

$$I = I_1 + I_2 + I_3. \tag{15}$$

Since there are many coefficients in the transfer functions shown in equation (9) and (12), it is difficult to determine an appropriate controller directly. To obtain the optimal controller, in the present paper the following cost function is presented:

$$J = \int_0^{\Omega} [h_1 w(\omega)^2] \, \mathrm{d}\omega, \tag{16}$$

where h_l are the weights, and Ω are the upper values of the frequency considered in the design of the controller. For vibration control, it is important to reduce the resonance peaks in the frequency region. Equation (16) denotes the square of the displacement, so if equation (16) is minimized, the frequency response curve becomes flat in the frequency domain. This implies that the vibration can be controlled to be small in the wide frequency zone. Since the equation of state is non-linear, as mentioned above, it is difficult to obtain the optimal values of the coefficients analytically, so that a numerical scheme is applied. The expression for obtaining the coefficient is

$$X_{lm} = X_{lm-1} - \eta(\partial J/\partial X_l) \qquad (m = 1, 2, \ldots, \infty), \tag{17}$$

where the X_l are the coefficients of the controller: $(X_1\ X_2\ X_3\ \ldots) = (d_1\ d_2\ c_1\ \ldots)$. The coefficients can be obtained by repeating the calculation of equation (17) with respect to m.

As an example, the optimal values of the coefficients are calculated for the vibration isolation control in the following case: the mass of the levitated body, $m = 0{\cdot}12$ kg, the amplitude of the base disturbance, $u_0 = 0{\cdot}2$ mm; and the initial air gap, $d = 2$ mm. The calculations are carried out for the same conductor as mentioned above in the same cooling condition. To design the controller, the relation between the control force and the current in the coil is required. The relations were obtained by experiment. The control force depends on the vibration amplitudes, so there is also the non-linear relationship between the control force and the vibration amplitudes. An example of the relationship obtained by the experiment is depicted in Figure 5. The non-linear relationship is expressed by the polynomial equations by using the least squares method, as shown in the solid and dotted lines in Figure 5. The expressions are used in the numerical calculation for obtaining the control forces. Since the equations given in equations (8)–(15) are non-linear, as just mentioned, the Runge–Kutta–Gill method is applied. The time response curves are calculated by the method, and the frequency response curve is obtained by taking the amplitudes in the steady state. Substituting the amplitudes versus frequencies into equation (16), and repeating the calculation of equation (17), one obtains the optimal coefficients of the controller. The maximum current is limited to within 5 A, corresponding to the capacity of the power amplifier used in the experiment, so the calculations are carried out under the limitation of the current being 5 A. In Table 3 are depicted optimal values of the coefficients, but the values of c_1 and c_2 are taken as constant values ($c_1 = c_2 = 1$) because the values do not affect the transfer functions, as shown in equation (9). The initial values for the coefficients before optimization are also depicted in Table 3. In the table, the coefficients vary significantly from the initial values. It can be seen that the variations in the coefficients d_1, d_2, g_1 and g_2 are large in comparison with c_2 and e_2. The theoretical response curve with the present optimal control or without control is depicted in Figure 6. In the figure, the curve before optimization (dotted line in Figure 6) is almost the same as that without control (chain line in Figure 6). However, when the optimal controller is utilized, the vibration (solid line in Figure 6) is reduced significantly across the whole frequency range. In particular, the vibration amplitude at low frequency is reduced significantly, and this cannot be controlled by the PID control. It can also be seen that the superharmonic peak due to non-linear vibration is reduced.

To validate the present control method, experimental tests were also carried out for the same model as just mentioned. In the experiment, the displacement of the base u and that of the levitated body w were detected by the non-contact displacement sensors (the laser gap sensors). The signals of displacement were input to a digital signal processor (DSP), and the velocities ($\dot{u}$, $\dot{w}$) were calculated by the DSP. The control current $I\ (= I_1 + I_2)$ was

calculated by using the following equation corresponding to the transfer function as mentioned above:

$$\frac{dI_1}{dt} = \frac{1}{c_1}[d_1\dot{u} + d_2u - c_2I_1],$$

$$\frac{dI_2}{dt} = \frac{1}{e_1}[g_1\dot{w}_2 + g_2w_1 - e_2I_2]. \tag{18}$$

Real time calculation of equation (18) was performed for the short time Δt by use of Euler's method in the DSP, but in which u, $\dot{u}$, w and $\dot{w}$ were the signals obtained by the sensors. The real time signal corresponding to the calculated current was created and input to the coil as shown in the block diagram (Figure 7). The frequency response curves obtained in the experiment are shown in Figure 8. The curve for the present control has a significantly smaller resonance peak in comparison with that without control. The vibration amplitudes are also smaller than those without control in a low frequency region (ω = 10–100 rad/s). In addition, the non-linear superharmonic motion is also reduced and is significantly small. Although there are a few discrepancies in the resonance frequencies, the theoretical results (Figure 6) and the experimental data (Figure 8) are in good agreement. Therefore, the present method and the analysis are applicable to the vibration control of superconducting levitation systems.

5. CONCLUSIONS

The vibration control of a superconducting levitation system is discussed in this paper. Since the system has non-linear phenomena, it is difficult to obtain the exact dynamic behavior of the levitation system. Hence a method of modelling of the system has been presented, and it is clarified that the modelling is valid for solving non-linear vibrations of the system. A method of vibration control has also been presented, in which a feedback current has frequency weighting. To optimize the feedback current, the square of the displacement of the levitated body was taken as a cost function. The optimal coefficients of the transfer function of the controller were obtained by minimizing the cost function. As an example, a vibration isolation problem was discussed, and both theoretical and experimental results were obtained. The vibration amplitudes of the levitated body with the present control were significantly reduced as compared with those without the control. Although the theoretical resonance frequency was somewhat smaller than the experimental one, the experimental and theoretical results were in good agreement. Therefore the present method has advantages for controlling non-linear systems such as the high-Tc superconducting levitation system.

REFERENCES

1. M. Murakami, H. Fujimoto, T. Taguchi, S. Gotoh, Y. Shiohara, N. Koshizuka and S. Tanaka 1990 *Japan*, *Journal of Applied Physics* **29**, 1991–1994. Large levitation force due to flux pinning YBaCuO superconductors fabricated by melt–powder–melt growth process.
2. R. Takahara, H. Ueyama and Y. Yotsuya 1992 *Electromagnetic Forces and Applications*. New York: Elsevier see p. 437. Load carrying capacity of superconducting magnetic bearings.
3. H. Higasa, N. Kawauchi, S. Nakamura and N. Ito 1994 *Advances in Superconductivity* **VI**, 1231–1236. Technological problems of superconducting magnetic bearing and construction of flywheel powder storage system.
4. T. Sugiura, H. Hashizume and K. Miya 1991 *International Journal of Applied Electromagnetic Materials* **2**, 183–196. Numerical electromagnetic field analysis of type II superconductors.

5. H. Hashizume, T. Sugiura, K. Miya, Y. Ando, S. Akita, S. Torii, Y. Kubota and T. Ogasawara 1991 *Cryogenics* **31**, 601–606. Numerical analysis of coupling loss in superconductors.
6. M. Uesaka, Y. Yoshida, N. Takeda and K. Miya 1993 *International Journal of Applied Electromagnetic Materials* **4**, 13–25. Experimental and numerical analysis of three dimensional high-Tc superconducting systems.
7. M. Tsuchimoto, T. Honma, N. Takeda, M. Uesaka and K. Miya 1993 *Eng. Anal. Boundary Elements* **11**, 171–175. An axisymmetric boundary element analysis of levitation force on high-Tc superconductor.
8. M. Tsuchimoto, H. Takeuchi and T. Honma 1994 *Transactions of the IEEE Japan* **114-D**, 741–745. Numerical analysis of levitation force on a high-Tc superconductor for magnetic field configuration.
9. Y. Yoshida, M. Uesaka and K. Miya 1994 *International Journal of Applied Electromagnetic Materials* **5**, 83–89. Dynamic magnetic force analysis of high-Tc superconductor with flux flow and creep.
10. K. Nagaya 1996 *IEEE Transactions on Magnetics* **32-2**, 445–452. Analysis of a high-Tc superconducting levitation system with vibration isolation control.
11. K. Nagaya and S. Shuto 1996 *IEEE Transactions on Magnetics* **32-3**, 1888–1896. Approximate boundary conditions in a circular conductor and their application to nonlinear vibration analyses of high-Tc superconducting levitation system.
12. K. Nagaya and M. Ishikawa 1995 *IEEE Transactions on Magnetics*, **31-1**, 885–896. A non-contact permanent magnet levitation table with electromagnetic control and its vibration isolation method using direct disturbance cancellation combining optimal regulators.
13. K. Nagaya and N. Arai 1991 *Transactions of the American Society of Mechanical Engineers*, *Journal of Dyn. Sys. Meas. Contr.* **113**, 472–478. Analysis of permanent magnet levitation actuator with electromagnetic control.